

The Design of a Parabolic Reflector System with High Tracking Tolerance for High Solar Concentration

Katie Shanks^{1*}, Nabin Sarmah¹, K. S. Reddy² and Tapas Mallick¹

¹Environmental and Sustainability Institute, University of Exeter Penryn Campus, Penryn, TR10 9FE, UK
²Heat Transfer and Thermal Power Laboratory, Department of Mechanical Engineering, Indian Institute of Technology Madras, Chennai 600 036, India

*Kmas201@exeter.ac.uk

Abstract. A compact high concentrating photovoltaic (HCPV) module based on cassegrain optics is proposed; consisting of a primary parabolic reflector, secondary reflector and homogeniser. The effect of parabolic curvatures, reflector separation distance and the homogeniser's height and width on the tracking tolerance has been investigated for optimisation. In this type of HCPV, the addition of a solid transparent homogeniser to the two stage reflector design greatly improves the tracking tolerance. Optical simulation studies show high optical efficiencies of 84.82 – 81.89 % over a range of ± 1 degree tracking error and 55.49% at a tracking error of ± 1.5 degrees.

Keywords: Solar Concentrator Design Optical Efficiency Optimization Tracking Error Tolerance Acceptance Angle

PACS: 88.40.-j, 88.40.F-; 88.40.fc; 88.40.fm; 88.40.fr; 88.05.Bc; 42.15.-i; 42.15.Dp; 42.15.Eq; 42.79.Bh; 42.79.Ek;

INTRODUCTION

The higher the concentration ratio of a solar concentrator system, the more dependent upon tracking accuracy it becomes as demonstrated by Tang et al. [1], Kudret et al. [2], Chiam et al. [3] and X. Li et al. [4]. Solar tracking tolerances for two staged reflecting high concentration designs typically ranges between $\pm 0.1^\circ$ to $\pm 0.6^\circ$ [5-7] but with the addition of a flux homogeniser this can be greatly improved as shown by Gordon et al.[8,9] and McDonald et al. [10]. The two main aims of solar concentration systems are to reduce the cost of solar power by replacing expensive photovoltaic material with relatively cheap optical devices, and to increase the efficiency limit of single junction and multi-junction solar cells [6, 11]. However, with an increase in concentration ratio, the solar tracking accuracy required also increases, resulting in the need for expensive tracker systems which offset the cost benefit.

This study has been undertaken to understand in greater detail the contribution parameters within the cassegrain design make on the systems tracking tolerance. A parabolic type solar concentrator was optimized through Monte Carlo ray trace analysis to obtain $>80\%$ optical efficiency (including reflection and absorption losses) and a well distributed irradiance upon the receiver over a range of $\pm 1^\circ$ tracking error. The optical efficiency is maintained $>55\%$ up to $\pm 1.5^\circ$ tracking error.

DESIGN CONCEPT

A two-stage reflector type concentrator was explored due to the advantages of compactness and having an upward facing receiver [5]. The basic design for this solar concentrator employs a Cassegrain set up as shown in Fig. 1 to produce a concentrated uniform irradiance distribution upon a solar cell placed in the base of the 1st reflector.

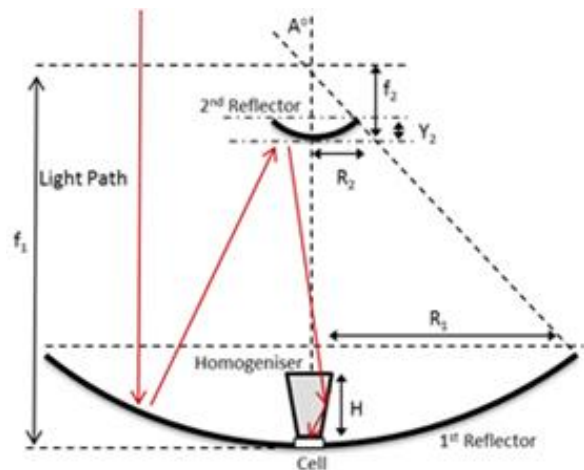


FIGURE 1, Theoretical light path through optics.

Light rays from the sun however have a divergence of $\pm 0.27^\circ$. This can be compensated for by separating

the focal points of both reflectors, so they are no longer coincident, and finding the optimum position of the secondary reflector with respects to the primary reflector and receiver.

The focal point, f , Radius, R , and depth, y , of a parabola are related through Eq. 1 [12].

$$R^2 = 4fy \quad (1)$$

It should also be noted that square cut parabolic reflectors were chosen for the primary collector to increase the packing factor when the primary reflectors are arranged side by side in an array system. In this way, the width, W , of a reflector is related to the radius, R , through Pythagoras and the width of the secondary reflector is referred to more than the radius in this research when ensuring all light rays are accommodated for. In Fig. 1 angle A is the maximum angle light can make with the vertical and still pass through the focal point.

It determines the utmost limit that light can strike the inside curve of the primary reflector and is related to the reflector's parabolic parameters via Eq. 3 [12].

$$\frac{f_1}{2R_1} = \frac{1}{4 \tan\left(\frac{A}{2}\right)} \quad (2)$$

The secondary reflector hence must be positioned or have a width that accommodates all rays. The width of the secondary reflector was chosen to be 50mm as a suitable size and weight that will not incur too much shadowing or difficulties in manufacturing and assembly. The following relationship was formed to calculate the separation distance (SD) between the two reflectors required to collect all rays given the secondary reflector width and primary collector focal length and radius:

$$SD = f_1 - \left(\frac{0.5W}{\tan\left(2 \tan^{-1}\left(\frac{R_1}{2f_1}\right)\right)} \right) \quad (4)$$

The radius of the primary reflector, R_1 , can also be dependent on the width, W , to ensure a concentration ratio of 500x is reachable when including the secondary reflector shadowing area.

SEPERATION DISTANCE

Combinations of varying primary and secondary reflector focal lengths were simulated first without the homogeniser, investigating the displacement of the

final ray positions due to a 1 degree tracking error. The separation distance was also changed, calculated using Eq. 4 above and taking the secondary reflector width, W , as 50mm.

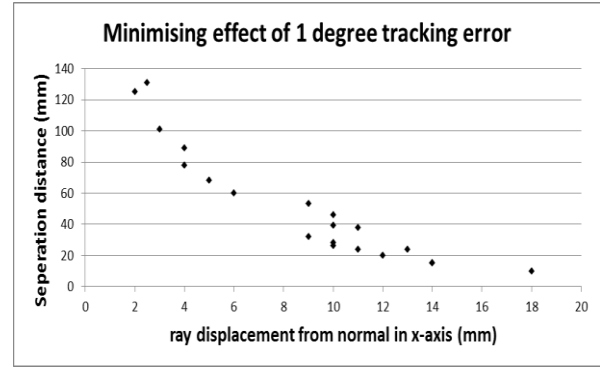


FIGURE 2, Separation distance vs. ray displacement from normal sun alignment due to 1° tracking error.

Larger separation distances result in lower ray displacement and hence a higher tracking tolerance as shown in Fig. 2. The separation distance is linked to the primary reflector focal length which counter intuitively must be decreased to gain larger separation distances. This is due to the need to converge the light rays to the cell size with the secondary reflector which entails increasing the secondary reflector focal length but then displacing it further from the primary reflector. However, this has limitations, including the width of the secondary reflector as mentioned earlier. The homogeniser was hence introduced as a means to let the rays focus and diverge before the receiver but still be redirected to the cell active area. The homogeniser is a crossed V-trough as shown in Fig. 3.

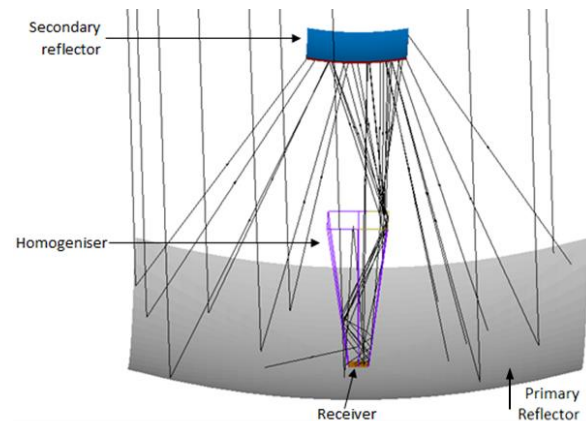


FIGURE 3, 3D ray trace diagram of incident rays at an angle of 1.5° and a solid transparent homogeniser with TIR within which catches otherwise lost rays.

HOMOGENISER

The focal lengths of the primary concentrator and secondary reflector were then investigated with a metal homogeniser (mirrored sides). The reflectivity of the sides were taken to be 95% and a shortlist of parameter combinations were found from various simulation testing and shown in Fig. 4 below.

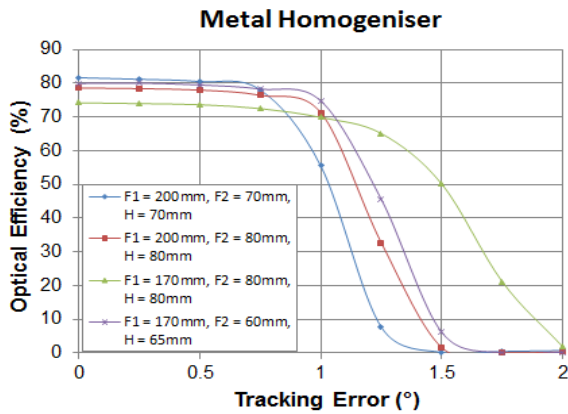


FIGURE 4, Optical Efficiency vs. tracking error. F1 and F2 are the focal lengths of 1st and 2nd reflectors, H represents the height of the homogeniser and SD represents the Separation Distance between the two reflectors.

The relatively low initial optical efficiency at normal incidence in Fig.4 is due to the reflection loss at the primary reflector, secondary reflector, and third stage homogeniser. The sharp decline in optical efficiency from 1 degree to 1.5 degrees seen is due to an increase in the number of reflections within the homogeniser, (reflective losses), and because of light passing by the homogeniser (diverging by > 10mm). The tracking tolerance can be improved by using a solid transparent homogenise utilising TIR and optimising the width. For this, the parameters obtaining the highest optical efficiency at normal incidence (F1 = 200mm, F2 = 70mm and H = 70mm from Fig 4.) were investigated further for optimisation as shown in Fig. 5.

Ideally the output face of the homogeniser, where the solar cell is placed, is the exact size of the cell active area to avoid loss. An output face of 10.1mm x 10.1mm was taken, instead of the 10mm x 10mm cell area, as a tolerance measure.

For maximum tracking tolerance, the light rays reflected from the secondary reflector should come to a focus upon entering the homogenisers input aperture and the input aperture width should be large enough to collect offset rays due to tracking errors. Increasing the width however also decreases the gradient of the

sloped sides, resulting in more rays not meeting the criteria for TIR. Various parameter combinations were investigated in an attempt to find the optimum scenario.

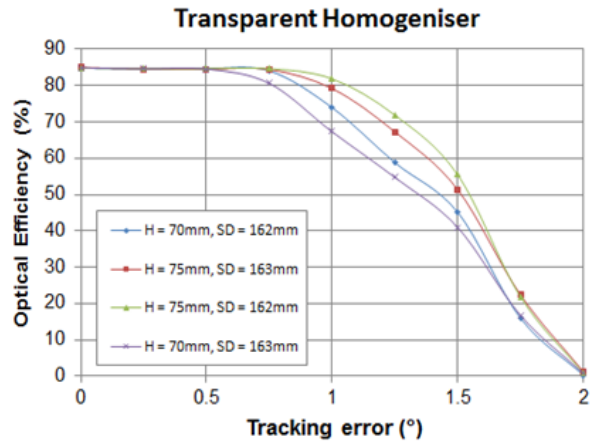


FIGURE 5, Graph of optimum parameter combinations for tracking tolerance. Entry aperture width = 30mm for all, H represents Homogeniser height and SD represents separation distance.

The most promising system parameter combination for tracking tolerance was chosen to be that with a homogeniser height of 75mm, an input width of 30mm and a separation distance between the two reflectors of 162mm. This configuration maintains an optical efficiency of 84.82 – 81.89 % over ± 1 degree tracking error and 55.49% optical efficiency at a tracking error of 1.5 degrees. The irradiance distribution of each set of parameter configurations was also recorded, all of which followed a similar trend with increasing tracking error as shown below in Fig. 6.

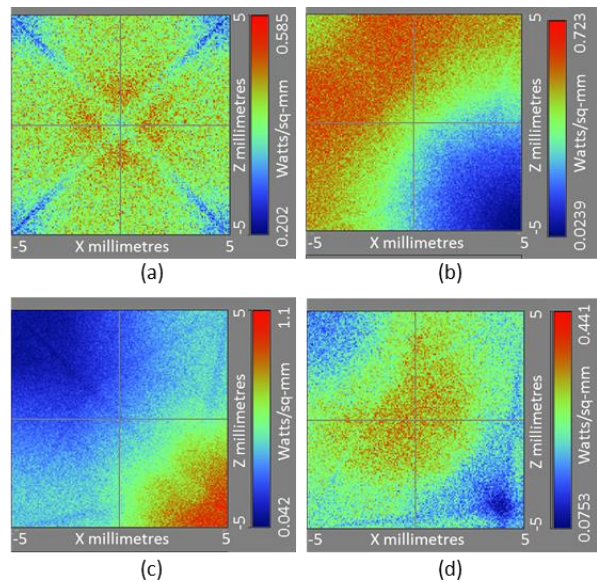


FIGURE 6, The irradiance distribution upon the receiver with increasing tracking error for the chosen system parameter configuration with: (a) No tracking error; (b) 0.5 degree tracking error; (c) 1 degree tracking error and (d) 1.5 degree tracking error.

ERROR ANALYSIS

The optical efficiency drops from 81.89% to 79.21% due to a ± 1 mm vertical error at a tracking error of $\pm 1^\circ$. These as well as the accuracy of the homogenisers' exit aperture dimensions and its alignment with the cell are the main sources of loss for this design.

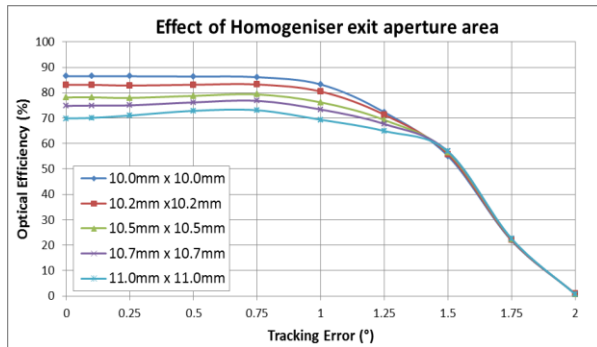


FIGURE 7, Decrease in optical efficiency due to mismatch of exit aperture area and cell area.

Perfect alignment with the cell and a homogeniser exit aperture of 10 x 10 mm obtains a maximum of 86.46% optical efficiency. With a 0.1mm alignment tolerance, the exit aperture dimensions, 10.1mm x 10.1mm, produces a maximum of 84.82% optical efficiency and decreases by $\sim 1.7\%$ (absolute value) for every 0.1mm increase in the area dimensions.

CONCLUSION

The tracking tolerance and optical efficiency of a cassegrain type solar concentrator was optimized through the use of monte carlo ray tracing to achieve high optical efficiencies of 84.82% (including reflection and absorption losses) at normal incidence, 81.89% at $\pm 1^\circ$ tracking error and 55.49% at $\pm 1.5^\circ$ tracking error. The optimized design was found to be with a primary parabolic reflector of focal length 200mm and a secondary inverse parabolic reflector of focal length 70mm placed 162mm from the primary collector. The optimized system required a solid transparent homogeniser of height 75mm with an entry aperture of 30mm x 30mm and exit aperture of 10.1mm by 10.1mm. The parameter relationships given, such as the equation for separation distance would be useful even as a preliminary stage in

optimisation processes of two stage reflecting systems utilising a parabolic primary. The detailed analysis of the proposed system may be beneficial in the design of parabolic reflector systems, as well as single stage lens systems (that focus onto a homogeniser), as a guideline to help improve an aspect of the system dependent on alignment, focusing area or uncertainties.

ACKNOWLEDGMENTS

This work has been carried out as part of the BioCPV project jointly funded by DST, India and EPSRC, UK. Authors acknowledge both the funding agencies for the support.

REFERENCES

- Runsheng Tang, Xinyue Liu, "Optical performance and design optimization of V-trough concentrators for photovoltaic applications", *Sol. Energy*, **85**, 2154-2166, (2011). <http://dx.doi.org/10.1016/j.solener.2011.06.001>
- M.Kudret Selçuk, "Analysis, development and testing of a fixed tilt solar collector employing reversible vee-trough reflectors and vacuum tube receivers, *Sol. Energy*, **22**, 413-426, (1979).
- H.F. Chiam, "Bi-yearly adjusted V-trough concentrators", *Sol. Energy*, **28**, 407-412, (1982).
- X. Li, Y. J. Dai, Y. Li, and R. Z. Wang, "Comparative study on two novel intermediate temperature CPC solar collectors with the U-shape evacuated tubular absorber", *Sol. Energy*, **93**, 220-234, (2013).
- Luque-Heredia, J.M. Moreno, P.H. Magalhaes, R. Cervantes, G. Quemere, and O. Laurent, "Inspira's CPV Sun Tracking", in *Concentrator Photovoltaics*, A. Luque, and V. Andreev, ed. (Springer Series in Optical Sciences, **130**, 221-250, (2007).
- J.M. Gordon, "Concentrator Optics", in *Concentrator Photovoltaics*, A. Luque, and V. Andreev, ed. (Springer Series in Optical Sciences, **130**, 113-132, (2007).
- A. Akisawa, M. Hiramatsu, and K. Ozaki, "Design of dome-shaped non-imaging Fresnel lenses taking chromatic aberration into account," *Sol. Energy*, **86**, 877-885, (2012).
- Jeffrey M. Gordon ; Daniel Feuermann ; Pete Young; Maximum-performance photovoltaic concentration with unfolded aplanatic optics. Proc. SPIE 7043, High and Low Concentration for Solar Electric Applications III, 70430D (September 09, 2008); doi:10.1117/12.792229.
- Alex Goldstein and Jeffrey M. Gordon, "Double-tailored nonimaging reflector optics for maximum-performance solar concentration," *J. Opt. Soc. Am. A* **27**, 1977-1984 (2010).
- Mark McDonald ; Chris Barnes; Spectral optimization of CPV for integrated energy output. Proc. SPIE 7046, Optical Modeling and Measurements for Solar Energy Systems II, 704604 (August 28, 2008); doi:10.1117/12.793447
- H. Doleman, "Limiting and realistic efficiencies of multi-junction solar cells", University of Amsterdam, (2012). Last accessed: 25/02/2014. <http://www.erbium.nl/publications/Masters%20theses/Master%20thesis%20Hugo%20Doleman%202012.pdf>
- Richard Aufmann, Vernon C. Barker and Richard Nation, *College Algebra and Trigonometry*, (Cengage Learning, 2010).